

Higgs Production and Decay from TeV Scale Black Holes at the LHC

Arif Emre Erkoca,^{1,*} Gouranga C. Nayak,^{1,†} and Ina Sarcevic^{1,2,‡}

¹*Department of Physics, University of Arizona, Tucson, AZ 85721, USA*

²*Department of Astronomy and Steward Observatory,*

University of Arizona, Tucson, AZ 85721, USA

(Dated: November 25, 2018)

Abstract

We perform detailed study of the Higgs production and decay, when Higgs is emitted from the black holes produced in proton-proton collisions at the Large Hadron Collider. We show that black hole production can significantly enhance the signal for the Higgs search at the LHC. We evaluate rapidity distribution of diphotons and transverse momentum distribution of bottom quarks, photons, tau leptons, top quarks and W bosons from Higgs decay, when Higgs is emitted from the black hole and also in case when these particles are produced directly from the black hole evaporation. We compare our results with the standard model backgrounds. We find that Higgs production from black holes is dominant over standard model production for $p_T^H > 100$ GeV, when $M_P = 1$ TeV. Diphotons from Higgs, when Higgs is produced from evaporation of black holes, are dominant over the standard model prediction, for diphoton rapidity $|y_{\gamma\gamma}| \leq 1$, while bottom quarks are dominant over QCD background for large bottom quark transverse momentum, $p_T^b > 300$ GeV, when $M_P = 1$ TeV. We show that measurements of the photon and bottom quark transverse momentum distribution can provide valuable information about the value of the fundamental Planck scale. We also propose a new signal for black hole production at the LHC, an onset of increasing transverse momentum distribution of bottom quarks with large transverse momentum.

PACS numbers: PACS: 12.38.-t, 12.38.Cy, 12.38.Mh, 11.10.Wx

*Electronic address: aerkoca@physics.arizona.edu

†Electronic address: nayak@physics.arizona.edu

‡Electronic address: ina@physics.arizona.edu

I. INTRODUCTION

An idea for solving the so-called hierarchy problem was proposed by assuming the existence of large extra dimensions, in which only the gravity can propagate [1]. In this model, all ordinary matter is restricted to reside on a 3+1-dimensional brane and the only fundamental energy scale is taken to be of the order of TeV. In the presence of these large extra dimensions, the gravitational interaction between two massive particles can be modified through the definition of a higher dimensional Planck scale (M_P), which is related to the four dimensional Planck scale (M_{Pl}) by

$$M_{Pl}^2 = M_P^{n+2}(2\pi R)^n \quad (1)$$

with R being the size of each of these extra dimensions and n being the number of extra dimensions. When $M_P = 1TeV$ and n is ranging from 2 to 7, R extends from 1 mm to 1 fm [2]. The collider experiments and astronomical data have put constraints on the parameters n and M_P [3, 4]. For example, supernova cooling and neutron star heating by decay of gravitationally trapped Kaluza-Klein modes provide limits on M_P : $M_P \gg 1500$ TeV for $n = 2$, $M_P \gg 100$ TeV for $n = 3$, whereas for $n = 4$ ($n = 5$) supernova cooling yields $M_P > 4$ TeV ($M_P > 0.8$ TeV). In addition, nonobservation of black hole production by cosmic neutrinos provides the most stringent limit on M_P , i.e $M_P > 1 - 1.4TeV$ for $n \geq 5$.

One of the most striking consequences of a low fundamental Planck scale is the possibility of producing black holes and observing them in future colliders or in cosmic rays/neutrino interactions [5, 6, 7, 8, 9, 10, 11, 12]. At CERN's Large Hadron Collider (LHC) and in high energy cosmic ray and neutrino interactions, the collision of particles with trans-Planckian energies, i.e. energies larger than M_P , is achieved. The impact parameter of subatomic particles in this collision can be smaller than the n -dimensional Schwarzschild radius, thus making it possible for mini black holes to be produced. The black hole production cross section can be approximated with the geometrical cross section, $\sigma \sim \pi b^2 \sim \pi M_P^{-2}$, which corresponds to about 100pb for $M_P = 1TeV$. When the luminosity at the LHC reaches its peak value of $L = 10^{34} cm^{-2} s^{-1}$, this cross section corresponds to several million of events with black holes in one year of running.

Semi-classical approach restricts us to explore the parameter space where the mass of the black hole, M_{BH} , is much larger than the fundamental Planck mass, M_P . Around and

below this mass scale, quantum gravity effects become important. We will explore only the parameter space where the semi-classical approach is justified.

Once the black hole with mass larger than M_P is formed it quickly evaporates via Hawking radiation [13]. Since these black holes are very small in size (\sim a few $10^{-4} fm$), their temperatures are very high (~ 500 GeV - 1 TeV). Thus, they can emit heavy particles with masses less than their temperatures. The emission spectrum of these particles depends not only on their spin properties and energies but also on the structure of the spacetime. These effects can be described by the so-called “greybody factors” which define the effective area of the emitting body. Greybody factors were obtained for scalars, fermions and gauge bosons in the case for non-rotating [14] and rotating black holes [15].

One of the primary goals of the LHC is to search for the Higgs, particle which is responsible for generating masses of the particles in the Standard Model. The dominant channel for Higgs production in p-p collisions at LHC energies is via gluon fusion process. Subdominant contributions come from the quark antiquark and vector boson scatterings [16]. Since Higgs can not be detected directly at LHC the primary decay channel proposed for Higgs detection with ATLAS and CMS detectors is via diphoton production [17]. A discovery significance above 5 sigma is expected at LHC for Higgs with mass below 140 GeV for an integrated luminosity of 30 fb^{-1} . Higgs is expected to have mass above 114.4 GeV, which is the lower limit from the LEP data [18]. The Higgs discovery signal which consists of two isolated photons with high transverse momenta can be identified as a narrow peak at the Higgs mass on top of a continuous background. Other Higgs decay channels such as bottom quarks and tau leptons may be measured at LHC as well [19]. Compared to the diphoton channel, these decay channels have larger decay branching fractions in the range of Higgs mass considered, but they are experimentally challenging due to the presence of large QCD background [20].

Recently a new mode of Higgs production via Hawking radiation of black holes at LHC has been proposed [10]. In this paper we make a detailed calculation of the various decay channels of the Higgs emitted from the black hole, such as diphotons, bottom quarks, tau leptons, W bosons and top quarks. We also present results for the production of the same final state particles produced from the black hole evaporation. We compare our results with the corresponding Standard Model background processes.

The paper is organized as follows. In section II we describe production and the decay of black holes at LHC, including Higgs production from black holes. In section III we describe

the decay of the Higgs which is produced from black holes. In section IV we present the results and discussions and we conclude in section V.

II. PRODUCTION AND DECAY OF BLACK HOLES AT LHC

In the theories of large extra dimensions gravitational effects become stronger at distances which are less than the size of the extra dimensions and at trans-Planckian energies, mini black hole production becomes possible. The radius of the black holes depends on the mass of the black hole, number of extra dimensions and the fundamental Planck scale, [9]

$$R_{\text{BH}} = \frac{1}{\sqrt{\pi}M_P} \left(\frac{M_{\text{BH}}}{M_P} \frac{8\Gamma((n+3)/2)}{n+2} \right)^{\frac{1}{n+1}}, \quad (2)$$

The temperature of the black hole is inversely proportional to its radius, i.e.

$$T_{\text{BH}} = \frac{n+1}{4\pi R_{\text{BH}}}, \quad (3)$$

and its decay time is given by

$$\tau_{\text{BH}} = \frac{1}{M_P} \left(\frac{M_{\text{BH}}}{M_P} \right)^{\frac{n+3}{n+1}}. \quad (4)$$

Black hole decays emitting elementary particles with masses smaller than the temperature of the black hole, T_{BH} , via Hawking radiation, a process which has never been observed for astronomical black holes. The number of particles emitted from the black hole per unit time is given by [14]:

$$\frac{dN}{dt} = \frac{\sigma_G}{\exp(E/T_{\text{BH}}) \mp 1} \frac{d^3p}{(2\pi)^3} \quad (5)$$

where E and p are the energy and the momentum of the emitted particle and the spin statistics factor is -1 for bosons and +1 for fermions, σ_G is the greybody factor. In this paper, we use the geometrical optics limit for σ_G , i.e [21, 22, 23]:

$$\sigma_G = \pi \left(\frac{n+3}{2} \right)^{2/(n+1)} \frac{n+3}{n+1} R_{\text{BH}}^2. \quad (6)$$

The differential cross section for the standard model particles produced via the decay of the black holes is given by [24]

$$E \frac{d\sigma}{d^3p} = \frac{1}{(2\pi)^3 s} \sum_{a,b} \int_{(M_{\text{BH}}^{\text{min}})^2}^s dM_{\text{BH}}^2 \int_{\frac{M_{\text{BH}}^2}{s}}^1 \frac{dx_1}{x_1} f_a(x_1, Q^2) \hat{\sigma} f_b(x_2, Q^2) \frac{g p^\mu u_\mu \sigma_G \gamma^{\tau_{\text{BH}}}}{\exp(p^\mu u_\mu / T_{\text{BH}}) \mp 1}, \quad (7)$$

where $\hat{\sigma}$ is the parton level black hole production cross section which can be approximated with the pure geometrical form as $\hat{\sigma} \sim \pi R_{\text{BH}}^2$, Q is the factorization scale, f_a and f_b 's are the parton distribution functions, x_1 and x_2 are the momentum fractions of the colliding partons which satisfy $x_1 x_2 s = M_{\text{BH}}^2$, \sqrt{s} is the center of mass energy of the colliding hadrons, $M_{\text{BH}}^{\text{min}}$ is the minimum black hole mass, γ is the Lorentz factor, g is the number of internal degrees of freedom, and p^μ is the four momentum of the emitted particle

$$p^\mu = (\sqrt{m^2 + p_T^2} \cosh(y), p_x, p_y, \sqrt{m^2 + p_T^2} \sinh(y)) \quad (8)$$

and u^μ is the four velocity of the black hole, $u^\mu = (\gamma, 0, 0, \gamma v_{\text{BH}})$. Clearly u^μ satisfies $u^\mu u_\mu = 1$. In the center of mass frame, $\vec{p}_1 + \vec{p}_2 = 0$ and the momentum of the black hole becomes

$$\vec{P}_{\text{BH}} = (x_1 - x_2) \vec{p}_1, \quad (9)$$

where $\vec{P}_{\text{BH}} = \gamma M_{\text{BH}} \vec{v}_{\text{BH}}$ and \vec{p}_1 and \vec{p}_2 are the momenta of the colliding hadrons. If we assume that $p_1^\mu p_{1\mu} = 0$, and use the fact that $|\vec{p}_1| = \frac{\sqrt{s}}{2}$ we get

$$\gamma v_{\text{BH}} = \frac{(x_1 - x_2) \sqrt{s}}{2 M_{\text{BH}}}. \quad (10)$$

We find that the assumption of stationary black hole is reasonable because the cross sections calculated for the case of the stationary black hole ($v_{\text{BH}} = 0$) differs only by few percent from the cross section obtained by incorporating the effect of translational motion along the initial beam axis. This is due to the fact that not many black holes can reach relativistic speeds after they are formed. In addition, we make use of the identity

$$E \frac{d\sigma}{d^3p} \equiv \frac{d\sigma}{2\pi p_T dp_T dy} \quad (11)$$

to obtain the rapidity distribution, $\frac{d\sigma}{dy}$ and the transverse momentum distribution, $\frac{d\sigma}{dp_T}$, by integrating Eq. (7) for the particles directly emitted from the black hole.

III. DECAY OF HIGGS PRODUCED FROM EVAPORATION OF BLACK HOLES

To evaluate differential distributions of standard model particles from Higgs decay when the Higgs is emitted from the black hole, we fold the decay distribution of the Higgs with the differential decay rate for the decay mode considered:

$$E_1 E_2 \frac{d\sigma}{d^3 p_1 d^3 p_2} = \int \frac{d^3 p}{E} \left(E \frac{d\sigma}{d^3 p} \right)_{\text{BH} \rightarrow \text{H}} \left(\frac{B}{\Gamma} E_1 E_2 \frac{d\Gamma}{d^3 p_1 d^3 p_2} \right)_{\text{H} \rightarrow 1+2}, \quad (12)$$

where Γ is the decay rate, B is the decay branching fraction, subscripts 1 and 2 refer to the decay products, E and $p = |\vec{p}|$ are the energy and the momentum of the Higgs, respectively ($E = \sqrt{p^2 + m_H^2}$). From Eq. (12), one can obtain the differential cross section for one of the decay products with mass m :

$$E_1 \frac{d\sigma}{d^3 p_1} = \frac{B}{p_1 \sqrt{1 - 4m^2/m_H^2}} \int_{E_{\min}}^{E_{\max}} \left(E \frac{d\sigma}{d^3 p} \right)_{\text{BH} \rightarrow \text{H}} dE. \quad (13)$$

where $\left(E \frac{d\sigma}{d^3 p} \right)_{\text{BH} \rightarrow \text{H}}$ is given by Eq. (7). The derivation of Eq. (13) is given in the Appendix in which we also show that the normalized decay distributions agree with those given in [25]. This suggests that regardless of the type of the decay mode, the final expressions (Eq. (13)) for the single particle differential cross section always take the same form.

Furthermore, by considering the change of variables:

$$Q^\mu = p_1^\mu + p_2^\mu \quad \text{and} \quad 2k^\mu = p_1^\mu - p_2^\mu, \quad (14)$$

it becomes possible to solve the integrals analytically in Eq. (12) which then leads us to a simple relation between the differential cross section for the pair produced from the decay of Higgs emitted from the black hole and that for the Higgs produced by the black hole:

$$Q^0 \frac{d\sigma}{d^3 Q} = B \left(E \frac{d\sigma}{d^3 p} \right)_{\text{BH} \rightarrow \text{H}}. \quad (15)$$

Using Eq. (11) we calculate distributions for the single particles and for the particle pairs by integrating Eq. (13) and Eq. (15), respectively.

IV. RESULTS AND DISCUSSIONS

In this section we present results of Higgs production and decay from black holes at LHC. We also show our results for several standard model particles produced directly from black hole evaporation. Given current experimental limits, we consider the scenarios with $n = 6$ and $M_P = 1 - 3$ TeV. Since quantum effect become important when the black hole mass is close to the Planck mass, we consider black holes with mass $M_{\text{BH}}^{\text{min}} \geq 3 M_P$. We check that black hole production cross section at LHC is not sensitive to the choice for the number of extra dimensions. However, we find that our results depend on the value of the Planck mass and the minimum black hole mass. We use CTEQ6M parton distribution [26] with the factorization scale equals to R_{BH}^{-1} where R_{BH} is the black hole radius. We compare our results with the corresponding standard model predictions and also discuss the dependence of our results on the parameters n and M_P .

A. Higgs Production at LHC

In Fig. 1 we present the total cross section for Higgs production from black holes as a function of the Higgs mass at LHC and we compare our result with that of the next-to-next-to-leading order pQCD [27] obtained in the Standard Model. We find that for the Planck mass $M_P = 1\text{TeV}$, and the minimum black hole mass, $M_{\text{BH}}^{\text{min}}=3 M_P$, the Higgs production cross section from black holes at the LHC is much larger than the Standard Model prediction. This is qualitatively consistent with the result in [28], which was obtained with fixed black hole mass. Therefore, if black holes are produced at LHC, it will have a direct impact on Higgs search at LHC.

In Fig. 2 and Fig. 3 we present transverse momentum distributions of the Higgs, when Higgs is produced from black holes, compared with the Higgs produced via standard model processes obtained using next-to-leading order pQCD [29]. We note that transverse momentum distribution of Higgs from black holes increases as p_T increases, in sharp contrast to the result obtained from the standard model predictions where the transverse momentum distribution decreases as p_T increases. As we will exemplify later, this is not only true for Higgs production from black holes but also for any particle emitted from black holes. Therefore, if TeV scale black holes are produced at LHC then an important signature is the increase

of the transverse momentum distribution as p_T increases. The origin of this p_T dependence is the high black hole temperature (~ 500 GeV -1 TeV). If black holes are indeed produced at LHC, then the black hole physics will dominate over all standard model physics.

In addition, our results indicate that the Higgs production via Hawking's radiation crucially depends on the value of the Planck mass and the minimum black hole mass and only marginally on the number of extra dimensions. As a numerical example, increasing M_P from 1 TeV to 2 TeV and $M_{\text{BH}}^{\text{min}}$ from 3 TeV to 6 TeV results in a decrease of the cross section by two orders of magnitude. A further suppression, no more than 30%, also occurs when n is decreased from 6 to 5. The shape of the distribution, however, remains unchanged.

B. Higgs Decay at LHC

Since the Higgs can not be directly detected at the LHC, we focus on various decay modes of the Higgs emitted by the black holes such as diphotons, bottom quarks, tau leptons, W bosons and top quarks. We compare these results with the standard model predictions. We use expressions for various Higgs decay mode distributions derived in the previous section.

We first concentrate on the diphoton production. We find that the total cross section for diphoton production from Higgs is increased by a factor of five due to the black hole contribution, when compared to the Higgs decay into diphoton in the Standard Model [30]. This enhancement also becomes apparent in the normalized transverse momentum distribution (Fig. 4) and in the normalized rapidity distribution (Fig. 5). We find that in the central rapidity region, $-1 \leq y \leq 1$, and for $p_T > 100$ GeV, the contribution from the Higgs emitted from the black hole becomes dominant. Thus, the formation of TeV scale black holes at LHC can significantly impact Higgs search via diphoton measurements with ATLAS and CMS detectors at LHC. In this study, we also analyze the effect of the black hole on the transverse momentum distribution for single photon. We find that $p_T^\gamma > 1$ TeV region needs to be explored to observe this effect which dominates over the Standard Model background given in [31]. However, the direct photon production from the black hole can be dominant over the Standard Model processes even for $p_T > 250$ GeV (Fig. 6).

We also consider other decay channels of Higgs, such as $H \rightarrow b\bar{b}$ and $H \rightarrow \tau^+\tau^-$. In Fig. 7 we present transverse momentum distribution for bottom quarks produced both directly and via Higgs decay from black holes and we compare our results with that of next-to-leading

order pQCD [32]. We find that the bottom quark production is suppressed by a few orders of magnitude when M_P is increased from 1 TeV to 2 TeV. For $p_T > 200$ GeV bottom quarks emitted from black holes dominate over the ones produced from Higgs, when $M_P = 1$ TeV and for $M_{BH}^{min} = 3$ TeV. However, the background from pQCD processes [32] is significant for bottom quarks with transverse momentum below 300 GeV. When $M_P = 2$ TeV and $M_{BH} > 6$ TeV, the background remains dominant to even larger values of the transverse momentum. To illustrate dependence of the bottom quark transverse momentum distribution on the choice of M_{BH}^{min} , we show in Fig. 7 the bottom quark production from black holes via Hawking's radiation for different minimum black hole masses with Planck mass being fixed to 1 TeV. We find that the shape of the bottom quark distribution is the same, but the overall normalization is about one order of magnitude smaller for the case of $M_{BH}^{min} = 5$ TeV than it is for $M_{BH}^{min} = 3$ TeV .

In Fig. 8 we summarize our results including the τ lepton transverse momentum distributions for both direct and indirect (via Higgs decay) production from the black hole.

In summary, we note that in general there is an onset in the transverse momentum distributions for the particles produced directly from the black holes below 500 GeV of p_T regardless of the choice of M_P or M_{BH}^{min} whereas a sharp decrease in these distributions is expected in the Standard Model scenarios. This is due to the high black hole temperatures which greatly exceed the mass of the particles considered. This feature can be used as a potential signal for the black hole production at LHC. On the other hand, the cross sections for the decay products of Higgs emitted from the black holes are slowly decreasing with p_T which can still contribute more than the Standard Model predictions. Furthermore, for the direct production of the particles from the black hole, we observe that the shape of the distributions mainly depend on the spin statistics. In addition, for a given statistical distribution, the overall normalization turns out to be dependent mostly on the number of internal degrees of freedom, g , whereas the effect of the particle mass seems insignificant especially at high p_T . As an example, when $p_T=500$ GeV, $(\frac{d\sigma}{dp_T})_\gamma/(\frac{d\sigma}{dp_T})_{Higgs} = 3.139 \sim 3$ which is the ratio of the number of internal degrees of freedom for these particles.

C. Parametrization

Our results from the previous sections seem to present a universal behavior in the transverse momentum distributions not only for particles produced directly from the black hole (Set 1) but also for the decay products of Higgs emitted from the black hole (Set 2). For Set 1, the shapes of the distributions turned out to be mostly dependent on the spin statistics factor, and the overall normalizations on the number of internal degrees of freedom for a given spin statistic. From the analysis of Set 2, we observe that the main difference between the distributions is due to the distinct branching fractions of the Higgs decays as presented below:

In order to parameterize our results, we fit each resulting distribution with the polynomial function in the form

$$f(p_T) = N \times [A_0 + A_1 \times p_T + A_2 \times p_T^2]. \quad (16)$$

where N, A_0, A_1 and A_2 are the best fit parameters. In order to find them, we apply Chi-Squared statistics together with LEVENBERG-MARQUARDT minimization method. Table (1) and Table (2) present the values of these parameters. As it is seen from Table (1), we obtained the parameters for Set 1, at best, by considering two different momentum ranges (i.e $p_T < 500$ GeV and $p_T > 500$ GeV). However, we do not need to follow this procedure for Set 2. As a result, all the fits turn out to possess percentage errors $< 5\%$ in particular for $p_T > 100$ GeV below which they tend to become larger due to the effect of the particle mass.

According to the values of the best fit parameters and the corresponding errors, we can conclude that the distributions indeed follow a general trend ,while, the effect of particle mass becomes important at relatively low p_T and the fits have smaller percentage errors for particles with low mass. We also observe that the normalization parameters for Set 1 are just the number of internal degrees of freedom of the particles emitted from the black hole as noted in the previous section. Furthermore, we also find that the normalization parameters for Set 2 are the decay branching fractions of the modes considered in this paper. Our results are obtained for the model parameters: $n = 6$, $M_P = 1$ TeV and $m_H = 120$ GeV and in the transverse momentum range, $p_T < 1$ TeV.

Fit Parameters		bosons			fermions		
$p_T < 500\text{GeV}$	$A_0(\text{pb}/\text{GeV})$	1.823×10^{-2}			-1.560×10^{-2}		
	$A_1(\text{pb}/\text{GeV}^2)$	5.425×10^{-4}			2.903×10^{-4}		
	$A_2(\text{pb}/\text{GeV}^3)$	-5.786×10^{-7}			-1.819×10^{-7}		
$p_T > 500\text{GeV}$	$A_0(\text{pb}/\text{GeV})$	1.358×10^{-1}			-1.540×10^{-2}		
	$A_1(\text{pb}/\text{GeV}^2)$	6.185×10^{-5}			2.755×10^{-4}		
	$A_2(\text{pb}/\text{GeV}^3)$	-7.318×10^{-8}			-1.630×10^{-7}		
		photon	W	Higgs	tau	bottom	top
	$N(p_T < 500\text{GeV})$	3.00	2.94	0.96	2.00	6.00	5.95
	$N(p_T > 500\text{GeV})$	3.00	2.98	0.98	2.00	6.00	5.88
	Percentage Errors	1%	1%	2%	2%	2%	5%

TABLE I: Fit parameters for the transverse momentum distributions of the particles produced directly from black holes.

$A_0(\text{pb}/\text{GeV})$	3.899×10^{-1}		
$A_1(\text{pb}/\text{GeV}^2)$	-5.648×10^{-4}		
$A_2(\text{pb}/\text{GeV}^3)$	2.541×10^{-7}		
	photon	tau	bottom
N	0.00221	0.0629	0.684
Percentage Errors	2%	2%	2%

TABLE II: Fit Parameters for the transverse momentum distributions for the decay products of Higgs emitted from the black hole.

D. W Boson and Top Quark Production From Heavy Higgs, when Higgs is Emitted from Black Holes

When the Higgs is heavier than about 150GeV, its dominant decay channels are W^\mp (and Z^0) bosons and top quarks. In Fig. 9 we present transverse momentum distributions for W boson production from black holes and from the Higgs, when Higgs is emitted from black holes. We also compare our results with the pQCD W boson production [33]. We take Higgs mass equal to 170 GeV and W mass to be 80 GeV. Similar to our previous results,

W boson production from black holes is larger than that produced from the Higgs decay. The latter distribution increases up to about 100 GeV and then starts decreasing. while, the former one increases as p_T increases. Both distributions dominate over the Standard Model prediction, especially for $p_T > 300$ GeV. Similar conclusions can also be derived for the top quark production (Fig. 10). Here, we again compare our results with that of the pQCD calculation [34] and we take Higgs mass to be 500 GeV and top quark mass to be 173 GeV in our calculations.

V. CONCLUSIONS

In this paper we have studied Higgs production and decay, when Higgs is produced from black holes at LHC. If the fundamental Planck scale is near a TeV, then parton collisions with high enough center-of-mass energy at LHC produce black holes. Since the temperature of these black holes are very high (\sim TeV), we might expect to see Higgs production from black holes at LHC via Hawking radiation. We have made a detailed study of the Higgs production and decay from black holes at LHC. We have calculated transverse momentum distribution for diphotons, tau lepton, bottom quarks, W boson and top quark produced from black holes decay and also from Higgs from black holes at the LHC. We have compared our results with the corresponding standard model predictions. We have found that for Planck mass ≥ 1 TeV and black hole mass ≥ 3 TeV, the diphoton and bottom quark production from Higgs from black holes at LHC is much larger than the standard model predictions. Hence black hole production can significantly impact direct Higgs search at LHC. We have found that transverse momentum distribution of particle production from black holes increases as p_T increases. Therefore we suggest that a measurement of increase in transverse momentum distribution as p_T increases is a potential signature of black hole production at the LHC. In addition, we have also noted that the shape of the transverse momentum distributions differs depending whether the emitted particle is a boson or a fermion. We have discovered that the major effect comes from the number of internal degrees of freedom in determining the overall normalizations of the distributions for the particles which obey the same spin statistics; however, the particle mass has almost no effect. We have also presented some parametric results that can be useful for some other studies.

In our calculations, we have considered the evaporation of the non-rotating black holes.

It was shown in [15] that the geometrical optics limit for the greybody factors in the case for fast rotating black holes is a factor of 3 larger than the one we have used. It can also be shown that the temperature of the black holes remains almost the same in the case of rotation. Therefore, the inclusion of rotation would lead to an enhancement in our results at most by a factor of 3.

We have also studied different decay channels of the Higgs which are produced from black holes at LHC for different values of the Planck mass. A direct comparison of the differential distributions with the experimental data at LHC will provide valuable information about the value of the fundamental Planck mass. Since the diphoton production from Higgs from black holes at LHC is larger than the standard model predictions, when the fundamental Planck mass is below 3 TeV, it enhances the chance of detecting Higgs at LHC via diphoton measurements at ATLAS and CMS detectors.

Acknowledgments

We thank Nick Kidonakis and Ramona Vogt for providing us the data for the cross section of the top quark in pQCD. We also thank Tolga Güver, Peter Loch and Jack Smith for many useful discussions. This work was supported in part by Department of Energy under contracts DE-FG02-04ER41319 and DE-FG02-04ER41298.

APPENDIX A: HIGGS DECAY RATES

In this section, we present our derivation of Eq. (13). We first start with the differential decay rate distributions of Higgs decaying into any two-body final states in the laboratory frame.

Decay distribution for any two-body decay of Higgs, i.e $H \rightarrow X\bar{X}$ is given by

$$\frac{d\Gamma}{d^3p_1 d^3p_2} = \frac{1}{(2\pi)^2} \frac{1}{8EE_1E_2} \delta^3(\vec{p}_1 + \vec{p}_2 - \vec{p}) \delta(E_1 + E_2 - E) |M|^2 \quad (\text{A1})$$

where 1 and 2 refer to the decay products both of which have mass m , $|M|^2$ is the spin averaged invariant decay amplitude squared and E , $p = |\vec{p}|$ and m_H are the energy, momentum and the mass of the Higgs respectively. After integrating over the momentum p_2 we get

$$\frac{d\Gamma}{d^3p_1} = \frac{1}{(2\pi)^2} \frac{1}{8EE_1E_2} \delta(E_1 + E_2 - E) |M|^2 \quad \text{and} \quad \vec{p} = \vec{p}_1 + \vec{p}_2 \quad (\text{A2})$$

We take the z-axis to be along the direction of \vec{p} and write $d^3p_1 = 2\pi\sqrt{E_1^2 - m^2}E_1dE_1d(\cos\theta)$. Using the properties of the delta function, we solve the angular part of the integration and obtain

$$\frac{d\Gamma}{dE_1} = \frac{|M|^2}{16\pi Ep} \quad \text{and} \quad E_- < E_1 < E_+ \quad (\text{A3})$$

where

$$E_{\mp} = \frac{E \mp p\sqrt{1 - 4m^2/m_H^2}}{2} \quad (\text{A4})$$

Eq. (A3) is a flat differential decay rate distribution with respect to the energy of one of the final state particles. Thus, the momentum and the energy conserving delta functions restrict the energy range of the final state particle for a given energy of the Higgs.

Since $|M|^2$ is independent of E_1 , it is simple to integrate over the energy E_1 and obtain the decay rate for a given mode:

$$\Gamma(E) = \frac{|M|^2}{16\pi Ep} \Delta E_1, \quad (\text{A5})$$

where ΔE_1 is the range of E_1 that can be calculated by using Eq. (A4).

From the Eqs. (A3) and (A5) we obtain the normalized decay rate energy distribution

$$\frac{B}{\Gamma} \frac{d\Gamma}{dE_1} = \frac{B}{p\sqrt{1 - 4m_f^2/m_H^2}} \quad (\text{A6})$$

where B is the decay branching fraction of the mode. This result satisfies the normalization condition given in [25]. This suggests us that we use the decay rate distribution in the following normalized form;

$$\frac{B}{\Gamma} \frac{d\Gamma}{d^3p_1} = \frac{B}{2\pi E_1 E_2} \frac{\delta(E_1 + E_2 - E)}{\sqrt{1 - 4m^2/m_H^2}} \quad (\text{A7})$$

In this paper, we calculate the differential cross section for the Standard Model particles produced from the decay of Higgs which is emitted from the black holes at the LHC. In order to find the single particle distribution we start with the equation

$$E_1 \frac{d\sigma}{d^3p_1} = \int \frac{d^3p}{E} \left(E \frac{d\sigma}{d^3p} \right)_{\text{BH} \rightarrow \text{H}} \left(\frac{B}{\Gamma} E_1 \frac{d\Gamma}{d^3p_1} \right)_{\text{H} \rightarrow 1+2}. \quad (\text{A8})$$

With a help of Eq. (A7) we get

$$E_1 \frac{d\sigma}{d^3p_1} = \int \frac{d^3p}{E} \left(E \frac{d\sigma}{d^3p} \right)_{\text{BH} \rightarrow \text{H}} \frac{B}{2\pi E_2} \frac{\delta(E_1 + E_2 - E)}{\sqrt{1 - 4m^2/m_H^2}}. \quad (\text{A9})$$

We assume that black holes produced in the proton-proton collisions remain stationary, and the spectrum of emitted particle then is spherically symmetric. We define the z-axis along the direction of \vec{p}_1 and write $d^3p = 2\pi p E dE d(\cos\theta)$ with θ being the angle between \vec{p} and \vec{p}_1 . Using the energy conserving delta function the angular integration leads to

$$E_1 \frac{d\sigma}{d^3p_1} = \frac{B}{p_1 \sqrt{1 - 4m^2/m_H^2}} \int_{E_{min}}^{E_{max}} \left(E \frac{d\sigma}{d^3p} \right)_{\text{BH} \rightarrow \text{H}} dE \quad (\text{A10})$$

where the limits of integration are

$$E_{min} = \left(\frac{E_1 - p_1 \sqrt{1 - 4m^2/m_H^2}}{2} \right) \left(\frac{m_H}{m} \right)^2 \quad (\text{A11})$$

$$E_{max} = \left(\frac{E_1 + p_1 \sqrt{1 - 4m^2/m_H^2}}{2} \right) \left(\frac{m_H}{m} \right)^2 \quad (\text{A12})$$

for $m \neq 0$ and

$$E_{min} = E_1 + \frac{4m_H^2}{E_1} \quad (\text{A13})$$

$$E_{max} = \infty \quad (\text{A14})$$

for $m = 0$.

-
- [1] N. Arkani-Hamed, S. Dimopoulos, G. Dvali, Phys. Lett. B **429**, 263 (1998); I. Antoniadis, N. Arkani-Hamed, S. Dimopoulos, G. Dvali, Phys. Lett. B **436**, 257 (1998); N. Arkani-Hamed, S. Dimopoulos, G. Dvali, Phys. Rev. D **59**, 086004 (1999); L. Randall and R. Sundrum, Phys. Rev. Lett. **83**, 3370 (1999); L. Randall and R. Sundrum, Phys. Rev. Lett. **83**, 4690 (1999).

- [2] G. Landsberg, *J. Phys. G* **32**, R337 (2006).
- [3] L. A. Anchordoqui, J. L. Feng, H. Goldberg, A. D. Shapere, *Phys. Rev. D* **68**, 104025 (2003);
B. Abbott *et al.* [D0 Collaboration], *Phys. Rev. Lett.* **86**, 1156 (2001); V. M. Abazov *et al.*
[D0 Collaboration], *Phys. Rev. Lett.* **90**, 251802 (2003).
- [4] K. Hagiwara *et al.* [Particle Data Group Collaboration], *Phys. Rev. D* **66**, 01001 (2002).
- [5] P. C. Argyres, S. Dimopoulos, J. March-Russell, *Phys. Lett. B* **441**, 96 (1998); T. Banks and
W. Fischler, *JHEP* **9906**, 014 (1999).
- [6] S. B. Giddings and S. Thomas, *Phys. Rev. D* **65**, 056010 (2002).
- [7] N. Akchurin *et al.*, [FERMILAB-FN-0752] (2004); S. Dimopoulos and G. Landsberg, *Phys.*
Rev. Lett. **87**, 161602 (2001); M. Cavaglia, R. Godang, L. M. Cremaldi, D. J. Summers,
JHEP **0706**, 055 (2007); V. Cardoso, M. Cavaglia, L. Gualtieri, *Phys. Rev. Lett.* **96** 071301
(2006); V. Cardoso, E. Berti, M. Cavaglia, *Class. Quant. Grav.* **22** L61-R84 (2005); L.
A. Anchordoqui, J. L. Feng, H. Goldberg, A. D. Shapere, *Phys. Lett. B* **594**, 363 (2004);
M. Cavaglia, *Int. J. Mod. Phys. A* **18**, 1843 (2003); T. G. Rizzo, *JHEP* **0202**, 011 (2002);
S. Nussinov and R. Shrock, *Phys. Rev. D* **59** 105002 (1999); J. L. Feng and A. D. Shapere,
Phys. Rev. Lett. **88**, 021303 (2002); L. A. Anchordoqui and H. Goldberg, *Phys. Rev. D* **65**,
047502 (2002); R. Emparan, M. Masip and R. Rattazzi, *Phys. Rev. D* **65**, 064023 (2002); S.
I. Dutta, M. H. Reno, I. Sarcevic, *Phys. Rev. D* **66**, 033002 (2002); L. A. Anchordoqui, J.
L. Feng, H. Goldberg, A.D. Shapere, *Phys. Rev. D* **66**, 103002 (2002); L. A. Anchordoqui,
J. L. Feng, H. Goldberg, A.D. Shapere, *Phys. Rev. D* **65**, 124027 (2002); A. Chamblin and
G.C. Nayak, *Phys. Rev. D* **66**, 091901 (2002); A. Chamblin, F. Cooper, G. C. Nayak, *Phys.*
Rev. D **70**, 075018 (2004); G. C. Nayak, [hep-ph/0806.4647]; K. Cheung, *Phys. Rev. D* **66**,
036007 (2002); M. Kowalski, A. Ringwald, H. Tu, *Phys. Lett. B* **529**, 1 (2002); A. Ringwald
and H. Tu, *Phys. Lett. B* **525**, 135 (2002); S. Hossenfelder, S. Holfmann, M. Bleicher,
H. Stocker, *Phys. Rev. D* **66**, 101502 (2002); R. Casadio and B. Harms, *Int. J. Mod. Phys.*
A **17**, 4635 (2002), *Phys. Rev. D* **64**, 024016 (2001), *Phys. Lett. B* **487**, 209 (2000).
- [8] R. Emparan, G. T. Horowitz, R. C. Myers, *Phys. Rev. Lett.* **85**, 499 (2000).
- [9] R. C. Myers and M. J. Perry, *Ann. Phys. (N.Y.)* **172**, 304 (1986).
- [10] S. Dimopoulos and G. Landsberg, *Phys. Rev. Lett.* **87**, 161602 (2001).
- [11] V. Cardoso, M. Cavaglia, L. Gualtieri, *Phys. Rev. Lett.* **96**, 071301 (2006); M. Cavaglia and
S. Das, *Class. Quant. Grav.* **21**, 4511 (2004); T. Han, G. D. Kribs, B. McElrath, *Phys. Rev.*

- Lett. **90**, 031601 (2003).
- [12] P. Meade and L. Randall, JHEP **0805**, 003 (2008).
- [13] S. W. Hawking, Commun. Math. Phys. **43**, 199 (1975).
- [14] P. Kanti, J. Grain, A. Barrau, Phys. Rev. D **71**, 104002 (2005); P. Kanti, Int. J. Mod. Phys. A **19**, 4899 (2004); C. M. Harris and P. Kanti, JHEP **0310**, 014 (2003); P. Kanti and J. March-Russell, Phys. Rev. D **67**, 104019 (2003); P. Kanti and J. March-Russell, Phys. Rev. D **66**, 024023 (2002).
- [15] S. Creek, O. Efthimiou, P. Kanti, K. Tamvakis, Phys. Lett. B **656**, 102 (2007); S. Creek, O. Efthimiou, P. Kanti, K. Tamvakis, Phys. Rev. D **76**, 104013 (2007); S. Creek, O. Efthimiou, P. Kanti, K. Tamvakis, Phys. Rev. D **75**, 084043 (2007); M. Casals, S. R. Dolan, P. Kanti, E. Winstanley, JHEP **0703**, 019 (2007); M. Casals, P. Kanti, E. Winstanley, JHEP **0602**, 051 (2006); C. M. Harris and P. Kanti, Phys. Lett. B **633**, 106 (2006); D. Ida, K. Oda, S. C. Park, Phys. Rev. D **73**, 124022 (2006), Phys. Rev. D **71**, 124039 (2005), Phys. Rev. D **69**, 049901 (2004); G. Duffy, C. Harris, P. Kanti, E. Winstanley, JHEP **0509**, 049 (2005).
- [16] M. Spira, [hep-ph/9510347]; A. Djouadi, J. Kalinowski, M. Spira, Comput. Phys. Commun. **108**, 56 (1998); G. Davatz, F. Stockli, C. Anastasiou, G. Dissertori, M. Dittmar, K. Melnikov, F. Petriello, JHEP **0607**, 037 (2006); C. Anastasiou, K. Melnikov, F. Petriello, Nucl. Phys. B **724**, 197 (2005); N. Kidonakis, Mod. Phys. Lett. A **19** 405 (2004); R. V. Harlander, W. B. Kilgore, Phys. Rev. Lett. **88**, 201801 (2002); S. Catani, D. de Florian, M. Grazzini, JHEP **0105** 025 (2001); S. Dawson, C. Kao, Y. Wang, P. Williams, Phys. Rev. D **75**, 013007 (2007).
- [17] CMS Collaboration, "The Compact Muon Solenoid Technical Proposal", CERN/LHCC 1994-38.
- [18] R. Barate *et al.*, Phys. Lett. B **565**, 61 (2003).
- [19] Peter Loch, private communications.
- [20] S. Ganjour, [hep-ex/0809.5163]; M. Takahashi, [hep-ex/0809.3224v2].
- [21] C. M. Harris and P. Kanti, JHEP **0310**, 014 (2003).
- [22] N. Sanchez, Phys. Rev. D. **16**, 937 (1977); Phys. Rev. D. **18**, 1030 (1978); Phys. Rev. D. **18**, 1798 (1978).
- [23] C. W. Misner, K. T. Thorne, J. A. Wheeler, Gravitation (Freeman, San Fransisco, 1973).

- [24] I. Mocioiu, Y. Nara, I. Sarcevic, Phys. Lett. B **557**, 87 (2003)
- [25] T. K. Gaisser, Cosmic Rays and Particle Physics (Cambridge University Press, New York, 1990).
- [26] J. Pumplin *et al.*, JHEP **0207**, 012 (2002).
- [27] V. Ravindran, J. Smith, W. L. van Neerven, Nucl. Phys. B **665**, 325 (2003).
- [28] G. C. Nayak and J. Smith, Phys. Rev. D **74**, 014007 (2006).
- [29] V. Ravindran, J. Smith, W. L. van Neerven, Nucl. Phys. B **634**, 247 (2002).
- [30] C. Anastasiou, L. Dixon, K. Melnikov, Nucl. Phys. Proc. Suppl. **116**, 193 (2003).
- [31] R. E. Blair, S. Chekanov, G. Heinrich, A. Lipatov, N. Zotov, [hep-ph/0809.0846v1].
- [32] P. Nason *et al.*, [1999 CERN Workshop], [hep-ph/0003142].
- [33] J. H. Kuhn, A. Kulesza, S. Pozzorini, M. Schulze, Nucl. Phys. **B797**, 27 (2008).
- [34] N. Kidonakis, R. Vogt, Phys. Rev. D **68**, 114014 (2003).

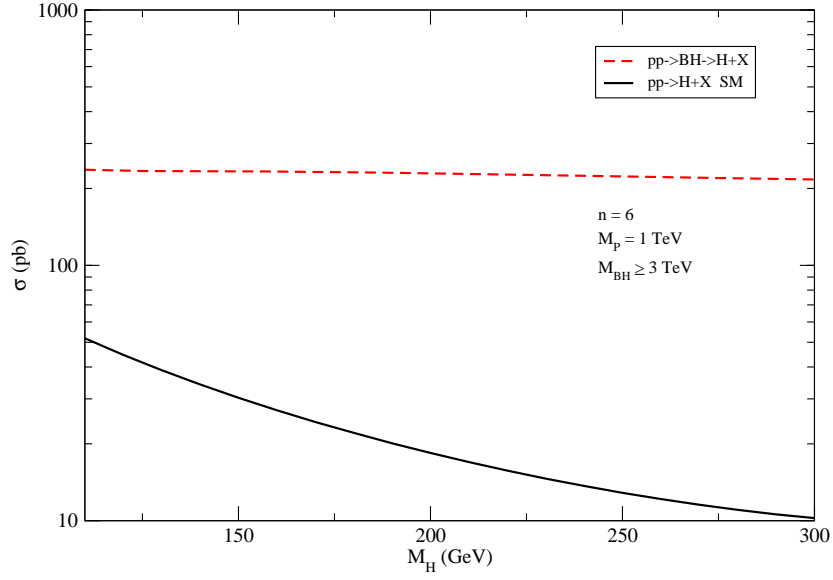


FIG. 1: Total cross section for the Higgs production from the black holes at LHC (dashed) compared with the standard model prediction (solid) [27] as a function of Higgs mass.

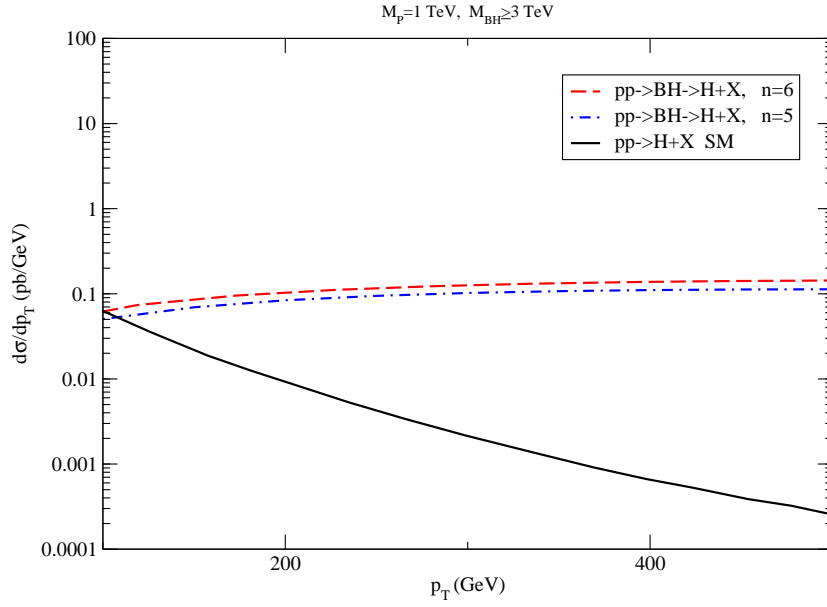


FIG. 2: Transverse momentum distribution for the Higgs with mass of 120 GeV produced by the black holes at LHC (dashed line) in a rapidity range $-2.5 < y < 2.5$ compared with the standard model result (solid line) [29].

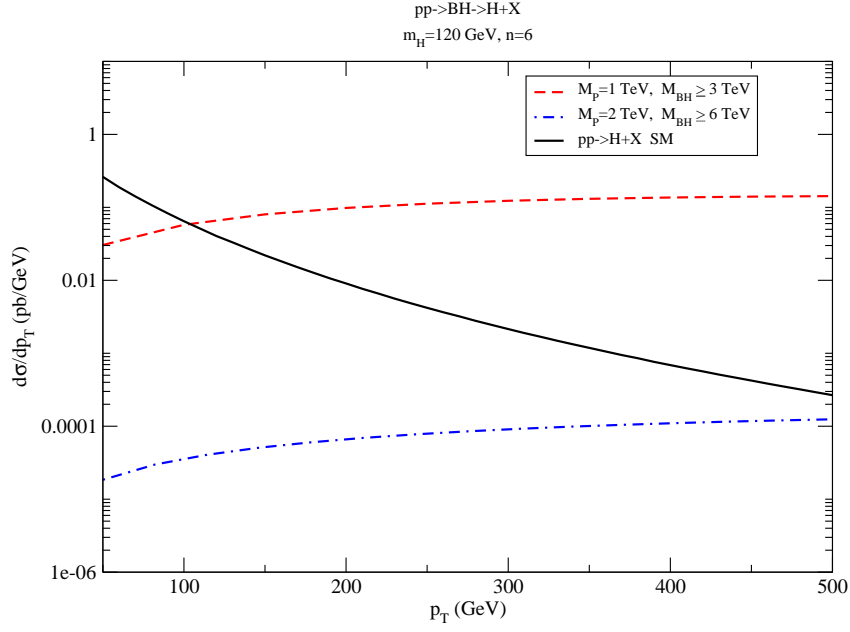


FIG. 3: Same as Fig.2 but for different values of the fundamental Planck masses and the minimum black hole masses; $M_P = 1 \text{ TeV}$ and $M_{\text{BH}}^{\text{min}} = 3 \text{ TeV}$ (dashed), $M_P = 2 \text{ TeV}$ and $M_{\text{BH}}^{\text{min}} = 6 \text{ TeV}$ (dot-dashed).

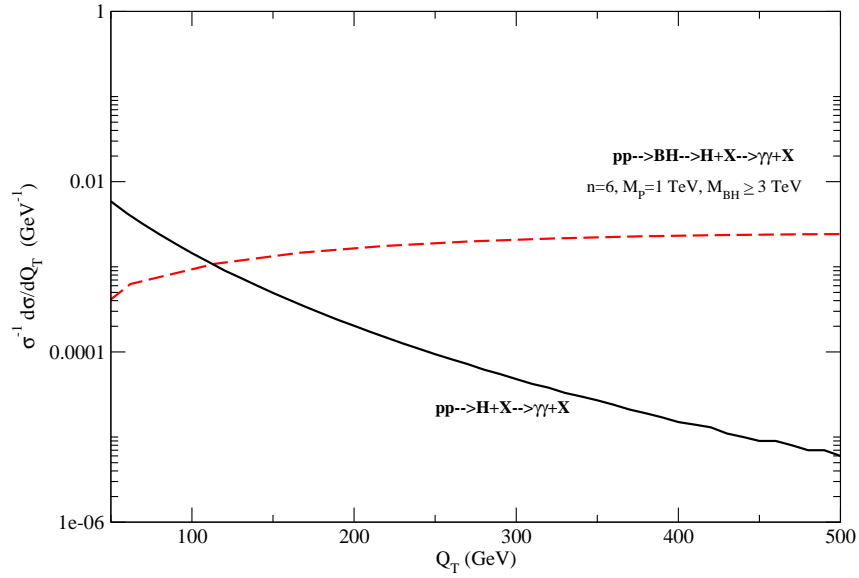


FIG. 4: Normalized transverse momentum distribution of diphoton pairs, when diphotons are emitted from the Higgs, produced in the Standard Model processes (solid line) [27, 29] and when the Higgs is emitted from black holes (dashed line).

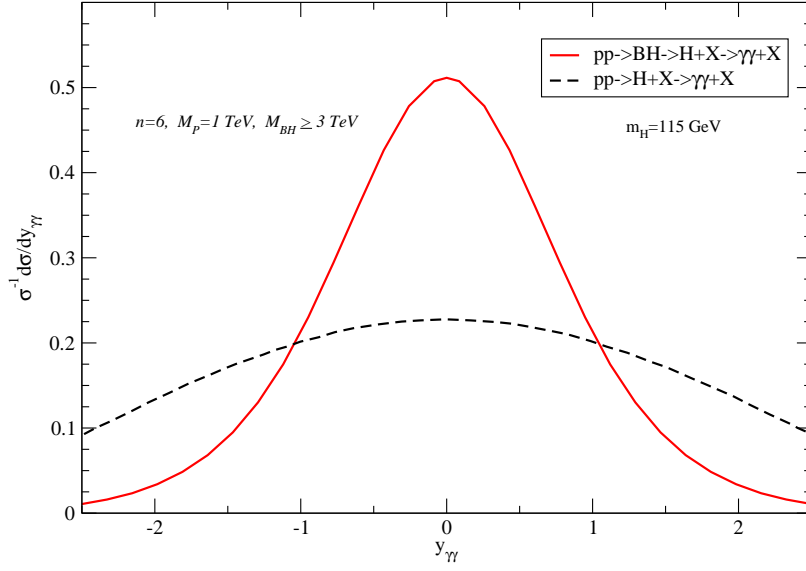


FIG. 5: Normalized rapidity distribution of the diphoton pairs, when diphotons are emitted from the Higgs, produced in the Standard Model processes (solid line) [30] and when the Higgs is emitted from black holes (dashed line).

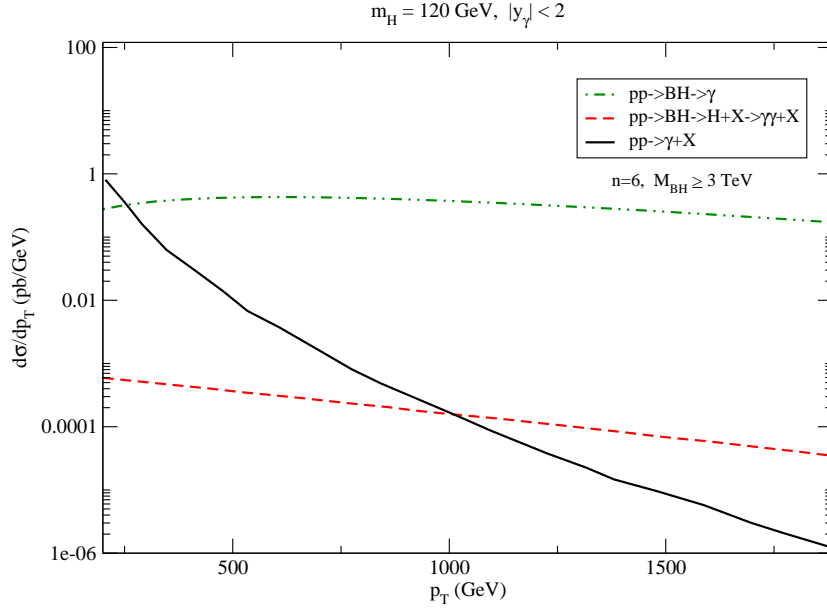


FIG. 6: Photon transverse momentum distribution, when photons are emitted from black holes (dot-dot-dashed line), when they are produced in Higgs decay, when the Higgs is emitted from black holes (dashed line) compared to the photons produced in the Standard Model [31].

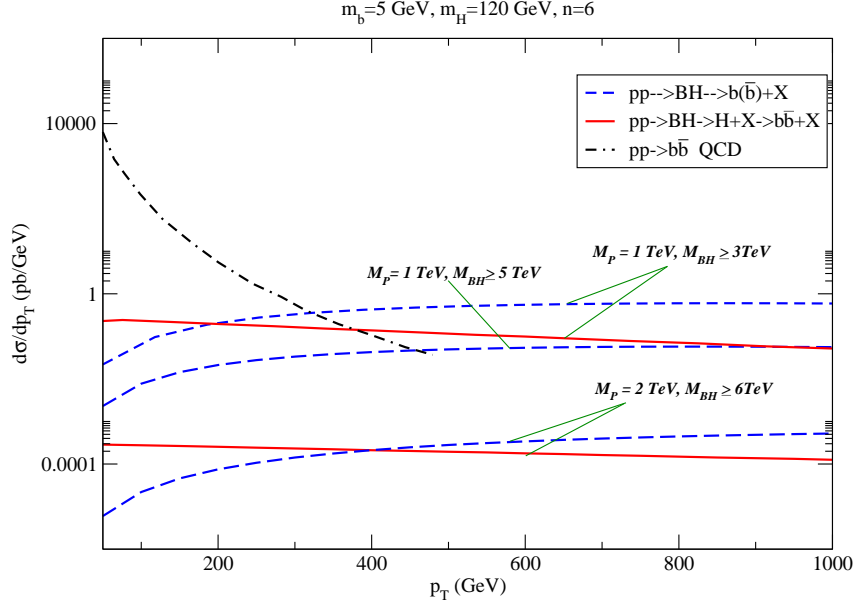


FIG. 7: Transverse momentum distribution for the bottom quarks produced from Higgs decay, when the Higgs is emitted from black holes (solid line), produced directly from black hole evaporation (dashed line) at the LHC. The upper (lower) curves correspond to the Planck mass of 1(2) TeV and minimum black hole mass of 3(6) TeV. The QCD prediction for bottom quark production is also presented (dashed-dot-dashed) [32].

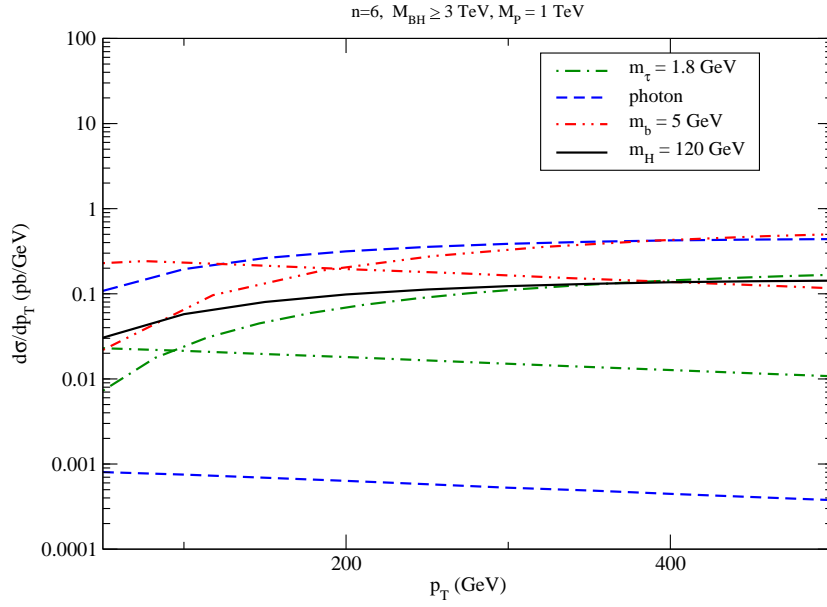


FIG. 8: Transverse momentum distribution distribution for the bottom quarks (dot-dot-dashed line), τ lepton (dot-dashed line), the Higgs (solid line) and single photon (dashed line). The upper curves at large p_T for each particle correspond to the direct production from black hole evaporation whereas the lower ones correspond to the decay of Higgs from black holes.

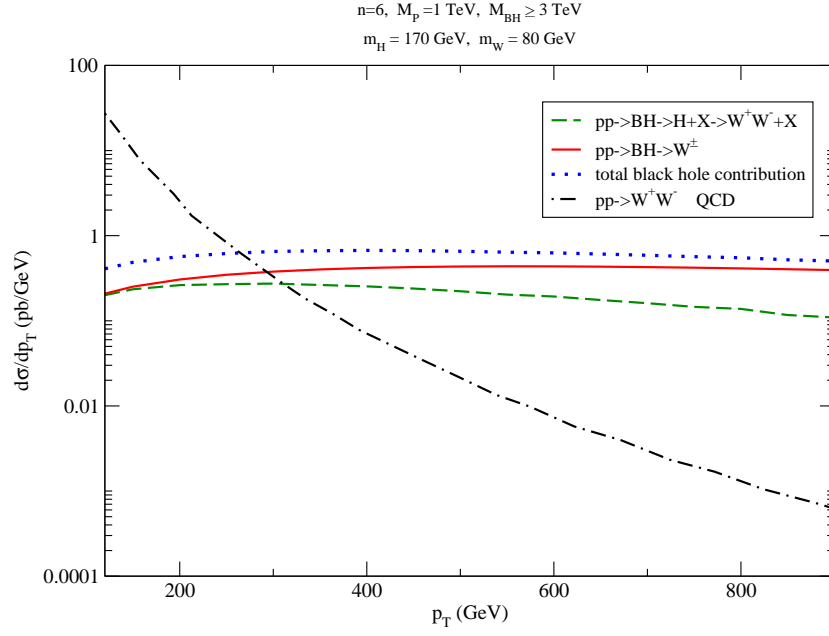


FIG. 9: Transverse momentum distributions for W boson produced from the the black hole (solid line) and from the Higgs, when Higgs is emitted from black holes (dashed line), compared with the Standard Model prediction (dash-dotted line) [33], the total black hole contribution is also shown (dotted line).

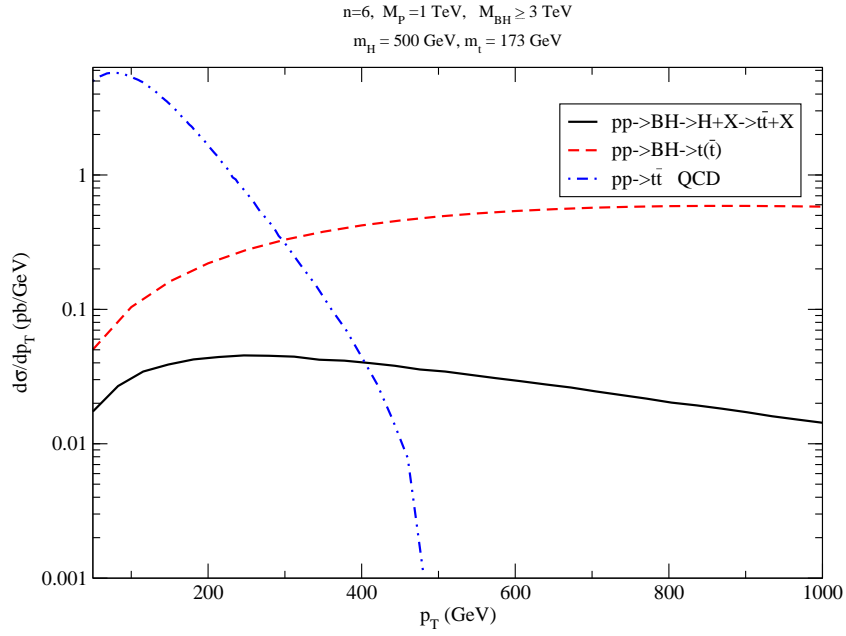


FIG. 10: Transverse momentum distributions for top quark emitted by black holes (dashed line) and from Higgs decay, when Higgs is emitted from black holes (solid line) compared with the QCD prediction (dotted line) [34].